Quadratic Mode Shape Components From Ground Vibration Testing

L. H. van Zyl
PhD Candidate
e-mail: lvzyl@csir.co.za

E. H. Mathews
Professor
Centre for Research and Continued Engineering Development,
North West University,
Suite 90, Private Bag X30,
0040 Pretoria, South Africa

Points on a vibrating structure generally move along curved paths rather than straight lines. For example, the tip of a cantilever beam vibrating in a bending mode experiences axial displacement as well as transverse displacement. The axial displacement is governed by the inextensibility of the neutral axis of the beam and is proportional to the square of the transverse displacement; hence the name "quadratic mode shape component." Quadratic mode shape components are largely ignored in modal analysis, but there are some applications in the field of modal-basis structural analysis where the curved path of motion cannot be ignored. Examples include vibrations of rotating structures and buckling. Methods employing finite element analysis have been developed to calculate quadratic mode shape components. Ground vibration testing typically only yields the linear mode shape components. This paper explores the possibility of measuring the quadratic mode shape components in a sine-dwell ground vibration test. This is purely an additional measurement and does not affect the measured linear mode shape components or the modal parameters, i.e., modal mass, frequency, and damping ratio. The accelerometer output was modeled in detail taking into account its linear acceleration, its rotation, and gravitational acceleration. The response was correlated with the Fourier series representation of the output signal. The result was a simple expression for the quadratic mode shape component. The method was tested on a simple test piece and satisfactory results were obtained. The method requires that the accelerometers measure down to steady state and that up to the second Fourier coefficients of the output signals are calculated. The proposed method for measuring quadratic mode shape components in a sine-dwell ground vibration test seems feasible. One drawback of the method is that it is based on the measurement and processing of second harmonics in the acceleration signals and is therefore sensitive to any form of structural nonlinearity that may also cause higher harmonics in the acceleration signals. Another drawback is that only the quadratic components of individual modes can be measured, whereas coupled quadratic terms are generally also required to fully describe the motion of a point on a vibrating structure.
[DOI: 10.1115/1.4005843]

Keywords: ground vibration testing, quadratic mode shape components

1 Introduction

The determination of the natural modes of vibration of a structure is required in many diverse applications, among others for the flutter analysis of new aircraft. This is often done using finite element analysis (FEA), but then is usually verified by a ground vibration test (GVT). In the majority of applications the linear mode shape components are sufficient. Quadratic mode shape components are however required for the modal-basis analysis of vibrations of rotating structures [1] and buckling [2]. Van Zyl and Mathews [3] also showed that the flutter prediction of aircraft with T-tails may be improved by including the quadratic mode shape components in the analysis.

Methods for determining the quadratic mode shape components from FEA have already been developed. Segalman et al. [4,5] used inertial loadings, obtained from a linear normal modes analysis, in nonlinear static analyses to extract the quadratic mode shape components. The use of nonlinear finite element analysis does not necessarily imply that the structure is nonlinear, but reflects on the inability of the linear finite element method to calculate; for example, the axial deflection of the tip of a cantilever beam under transverse load. Van Zyl and Mathews [6] used energy principles to obtain quadratic modes shape components from linear finite element analysis. The subject of this paper is the experimental determination of the parabolic approximation to the path described by a typical acceleration sensor used in a GVT.

In a sine-dwell or phase resonance GVT the structure is excited at each modal frequency using electromechanical exciters. The response is measured using a large number of accelerometers attached to the structure. The linear mode shape is determined from the first harmonic of the response, i.e., the harmonic component at the excitation frequency.

The accelerometers fixed to the structure generally experience rotation as well as linear acceleration. This rotating reference frame introduces coupling between the linear acceleration components at twice the excitation frequency; in addition to introducing coupling between gravity and linear acceleration at the excitation frequency. It will be shown that, despite this unwanted coupling, it is possible to resolve the curved path described by an accelerometer.

2 Derivation

2.1 Direct Measurement of Quadratic Mode Shape Components. We consider a triaxial accelerometer attached to a structure resonating in mode i, i.e., the whole structure is vibrating in phase. For the sake of simplicity we assume that the measurement axes of the accelerometer at rest are aligned with the global axes and that gravity acts in the negative z direction, i.e.,

$$\mathbf{g} = (0, 0, -g) \tag{1}$$

where $\mathbf{g}$ is the gravitational acceleration vector and g is the scalar gravity magnitude. Without consideration of the underlying physics we assume a parabolic approximation to the curved path followed by the accelerometer. With this assumption, the displacement and rotation of the accelerometer in terms of the generalized coordinate s_i are given by (cf. Eq. (4) of Dohrmann and Segalman [2])

$$\begin{aligned} \mathbf{u}(t) &= \mathbf{u}^i s_i(t) + \mathbf{g}^{ii}(s_i(t))^2 \\ \mathbf{r}(t) &= \mathbf{r}^i s_i(t) \end{aligned} \tag{2}$$

where $\mathbf{u}(t)$ and $\mathbf{r}(t)$ are the instantaneous displacement and rotation of the accelerometer, respectively. $\mathbf{u}^i$ is the linear modal displacement, $\mathbf{g}^{ii}$ is the quadratic modal displacement, and $\mathbf{r}^i$ is the modal rotation vector. It is assumed without loss of generality that the generalized coordinate varies as

$$s_i(t) = \cos \omega t \tag{3}$$

The instantaneous displacement, acceleration, and rotation can be derived from Eqs. (2) and (3) and the trigonometric identity $\cos^2\theta = \frac{1}{2}(1 + \cos 2\theta)$ as

Contributed by the Design Engineering Division of ASME for publication in the JOURNAL OF VIBRATION AND ACOUSTICS. Manuscript received April 28, 2011; final manuscript received December 12, 2011; published online April 23, 2012. Assoc. Editor: Walter Lacarbonara.

$$\begin{aligned}\mathbf{u}(t) &= \mathbf{u}^i \cos\omega t + \frac{1}{2}\mathbf{g}^{ii} + \frac{1}{2}\mathbf{g}^{ii}\cos 2\omega t \\ \ddot{\mathbf{u}}(t) &= -\omega^2 \mathbf{u}^i \cos\omega t - 2\omega^2 \mathbf{g}^{ii}\cos 2\omega t \\ \mathbf{r}(t) &= \mathbf{r}^i \cos\omega t\end{aligned} \tag{4}$$

The accelerometer outputs depend on the instantaneous acceleration and the instantaneous orientation of the accelerometer, viz.

$$\begin{aligned}a_x &= \mathbf{e}_x \cdot (\ddot{\mathbf{u}} - \mathbf{g}) \\ a_y &= \mathbf{e}_y \cdot (\ddot{\mathbf{u}} - \mathbf{g}) \\ a_z &= \mathbf{e}_z \cdot (\ddot{\mathbf{u}} - \mathbf{g})\end{aligned} \tag{5}$$

where a_x, a_y, and a_z are the scaled outputs from the accelerometer, $\mathbf{e}_x$, $\mathbf{e}_y$, and $\mathbf{e}_z$ are unit vectors aligned with the x, y, and z axes of the accelerometer, respectively, and $\ddot{\mathbf{u}}$ is the instantaneous acceleration of the accelerometer. It should be noted that even accelerometers that do not measure steady acceleration do respond to a change in orientation in a gravitational field. For the purposes of this discussion, however, it is assumed that the accelerometer does measure steady acceleration. The first order approximation to the instantaneous orientation of the accelerometer is given by

$$\begin{aligned}\mathbf{e}_x &= (1,0,0) + \mathbf{r}(t) \times (1,0,0) = \left(1, r_z^i \cos\omega t, -r_y^i \cos\omega t\right) \\ \mathbf{e}_y &= (0,1,0) + \mathbf{r}(t) \times (0,1,0) = \left(-r_z^i \cos\omega t, 1, r_x^i \cos\omega t\right) \\ \mathbf{e}_z &= (0,0,1) + \mathbf{r}(t) \times (0,0,1) = \left(r_y^i \cos\omega t, -r_x^i \cos\omega t, 1\right)\end{aligned} \tag{6}$$

The instantaneous accelerometer outputs can be derived from Eqs. (1), (4), (5), and (6) and the trigonometric identity $\cos^2\theta = \frac{1}{2}(1 + \cos 2\theta)$, and by neglecting third order terms, to be

$$\begin{aligned}a_x &= -\omega^2 u_x^i \cos\omega t - 2\omega^2 g_x^{ii}\cos 2\omega t - \frac{1}{2}\omega^2 r_z^i u_y^i - \frac{1}{2}\omega^2 r_z^i u_y^i \cos 2\omega t \\ &\quad + \frac{1}{2}\omega^2 r_y^i u_z^i + \frac{1}{2}\omega^2 r_y^i u_z^i \cos 2\omega t - r_y^i g\cos\omega t \\ a_y &= -\omega^2 u_y^i \cos\omega t - 2\omega^2 g_y^{ii}\cos 2\omega t - \frac{1}{2}\omega^2 r_x^i u_z^i - \frac{1}{2}\omega^2 r_x^i u_z^i \cos 2\omega t \\ &\quad + \frac{1}{2}\omega^2 r_z^i u_x^i + \frac{1}{2}\omega^2 r_z^i u_x^i \cos 2\omega t + r_x^i g\cos\omega t \\ a_z &= -\omega^2 u_z^i \cos\omega t - 2\omega^2 g_z^{ii}\cos 2\omega t - \frac{1}{2}\omega^2 r_y^i u_x^i - \frac{1}{2}\omega^2 r_y^i u_x^i \cos 2\omega t \\ &\quad + \frac{1}{2}\omega^2 r_x^i u_y^i + \frac{1}{2}\omega^2 r_x^i u_y^i \cos 2\omega t + g\end{aligned} \tag{7}$$

The accelerometer outputs can also be represented by second order Fourier series containing only cosine terms:

$$\begin{aligned}a_x &= A_{0x} + A_{1x}\cos\omega t + A_{2x}\cos 2\omega t \\ a_y &= A_{0y} + A_{1y}\cos\omega t + A_{2y}\cos 2\omega t \\ a_z &= A_{0z} + A_{1z}\cos\omega t + A_{2z}\cos 2\omega t\end{aligned} \tag{8}$$

By equating the expressions for the respective acceleration components in Eqs. (7) and (8) and grouping terms of the same harmonic, we arrive at a system of equations from which the modal displacement at the accelerometer can be solved.

$$\begin{aligned}-\frac{1}{2}\omega^2 r_z^i u_y^i + \frac{1}{2}\omega^2 r_y^i u_z^i &= A_{0x} \\ -\frac{1}{2}\omega^2 r_x^i u_z^i + \frac{1}{2}\omega^2 r_z^i u_x^i &= A_{0y} \\ -\frac{1}{2}\omega^2 r_y^i u_x^i + \frac{1}{2}\omega^2 r_x^i u_y^i + g &= A_{0z}\end{aligned} \tag{9}$$

$$\begin{aligned}-\omega^2 u_x^i - r_y^i g &= A_{1x} \\ -\omega^2 u_y^i + r_x^i g &= A_{1y} \\ -\omega^2 u_z^i &= A_{1z}\end{aligned} \tag{10}$$

$$\begin{aligned}-2\omega^2 g_x^{ii} - \frac{1}{2}\omega^2 r_z^i u_y^i + \frac{1}{2}\omega^2 r_y^i u_z^i &= A_{2x} \\ -2\omega^2 g_y^{ii} - \frac{1}{2}\omega^2 r_x^i u_z^i + \frac{1}{2}\omega^2 r_z^i u_x^i &= A_{2y} \\ -2\omega^2 g_z^{ii} - \frac{1}{2}\omega^2 r_y^i u_x^i + \frac{1}{2}\omega^2 r_x^i u_y^i &= A_{2z}\end{aligned} \tag{11}$$

Subtracting Eq. (9) from Eq. (11) results in a simplified set of equations for the quadratic modal displacements

$$\begin{aligned}-2\omega^2 g_x^{ii} &= A_{2x} - A_{0x} \\ -2\omega^2 g_y^{ii} &= A_{2y} - A_{0y} \\ -2\omega^2 g_z^{ii} &= A_{2z} - A_{0z} + g\end{aligned} \tag{12}$$

The linear mode shape component is usually solved from Eq. (10) by neglecting the gravitational terms. The validity of this approach depends on the frequency: it is generally acceptable at high frequencies but not at low frequencies. For small test pieces the orientation during the GVT can be chosen to minimize the effect of gravity, both on the actual behavior of the structure and the measurement error introduced by neglecting gravity. However, for larger structures like aircraft this is not feasible and other means must be employed to obtain the actual linear mode shape components of the low frequency modes.

Unlike the linear component, the quadratic component can be determined directly from Eq. (12). Furthermore, the quadratic displacement in a given direction can be determined solely from the corresponding accelerometer output and it is independent of the linear component. On the down side, the determination of the quadratic mode shape component depends on the measurement of the mean shift (A_0 terms) and second harmonic (A_2 terms) in the acceleration signals. These terms are generally small compared to the first harmonics. Material or geometric nonlinearities may also give rise to harmonics in the accelerometer signals, leading to spurious curved trajectories.

Under certain conditions, e.g., for shallow arches or buckled beams at appropriate sag levels or buckling levels, respectively, two-to-one internal resonances may be activated as described by Lacarbonara et al. [7,8]. These resonances would give rise to second harmonics in the accelerometer outputs, however, the resonances would also affect the measurement of the linear mode shape component. A possible remedy would be to attach masses to the structure in order to alter the frequency ratio of the participating modes. The effect of the masses can be removed analytically from the GVT results at a later stage.

In addition, the method can only determine the quadratic components of individual modes, whereas coupled quadratic terms, i.e., terms that are proportional to the product of two modal coordinates, are generally required to fully describe the curved trajectory of a point on a vibrating structure.

2.2 Gravity Correction. A stationary accelerometer in a gravitational field senses the same acceleration as it would sense in the absence of gravity under linear acceleration equal to –**g**. Any rotation of the accelerometer, apart from a rotation about an axis parallel to the gravity vector, will also be sensed by the accelerometer as a linear acceleration. The change in the gravity vector, in the reference frame of an accelerometer experiencing a rotation **r**, is given by

$$\Delta\mathbf{g} = \mathbf{g} \times \mathbf{r} \tag{13}$$

The apparent acceleration of the accelerometer due to its rotation in the gravitational field is given by

$$\mathbf{a} = -\Delta\mathbf{g} = -\mathbf{g} \times \mathbf{r} \tag{14}$$

The total acceleration sensed by the accelerometer, due to its linear acceleration and its rotation in the gravitational field, is given by

$$\mathbf{a} = \ddot{\mathbf{u}} - \mathbf{g} \times \mathbf{r} \tag{15}$$

For an accelerometer fixed to a structure resonating in mode i, the total apparent acceleration (disregarding the quadratic mode shape component) is given by

$$\mathbf{a} = -\omega^2 \mathbf{u}^i - \mathbf{g} \times \mathbf{r}^i \tag{16}$$

The apparent linear modal displacement $\tilde{\mathbf{u}}^i$ that would normally be derived from the accelerometer output according to Eq. (10) is therefore

$$\tilde{\mathbf{u}}^i = \mathbf{u}^i + \frac{1}{\omega^2}(\mathbf{g} \times \mathbf{r}^i) \tag{17}$$

It would be possible to remove the spurious component due to gravity if the rotation of each accelerometer was known. GVT data customarily includes node coordinate data, connectivity data, and nodal displacement data. The concept of nodes and connections is illustrated in Fig. 1. Nodes are the measurement positions on the structure, i.e., where the accelerometers are attached. Connections are lines drawn between nodes for visualization purposes and are not related to actual structural elements. The two end points of a connection are referred to as neighbors in the description that follows.

The rotation of a node is determined by minimizing, in a least squares sense, the difference between the measured relative displacements of the node and its neighbors, and the displacements resulting from a rigid rotation about the node of all the connections between the node and its neighbors. This procedure requires that the node and all its neighbors are not collinear.

The rotation of the nodes can be expressed as a linear combination of the nodal translations:

$$\{\mathbf{r}^i\} = [\mathbf{A}]\{\mathbf{u}^i\} \tag{18}$$

Where $\{\mathbf{r}^i\}$ and $\{\mathbf{u}^i\}$ are concatenations of the nodal rotation and displacement vectors, respectively, of all the nodes. The actual modal displacement can therefore be solved from

$$\{\mathbf{u}^i\} = \left[\mathbf{I} + \frac{1}{\omega^2}[\mathbf{g} \times \mathbf{A}]\right]^{-1} \{\tilde{\mathbf{u}}^i\} \tag{19}$$

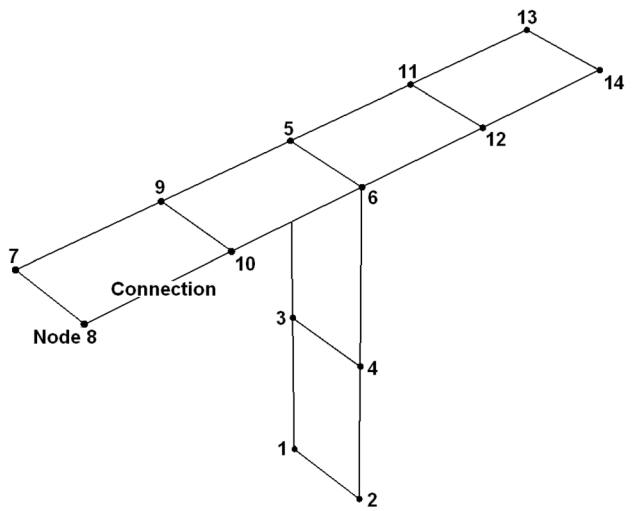

Fig. 1 Geometric model of a simple T-tail for visualizing GVT results

Where the matrix denoted by $[\mathbf{g} \times \mathbf{A}]$ is constructed as follows: The cross product with the vector $\mathbf{g}$ is expressed as a matrix multiplication by a 3×3 matrix. Each group of three rows of $\mathbf{A}$ is then multiplied through by this matrix.

This procedure does, however, amplify measurement errors and it is usually better to estimate the rotation from the measured mode shape, resulting in the alternative correction:

$$\{\mathbf{u}^i\} = \{\tilde{\mathbf{u}}^i\} - \frac{1}{\omega^2}[\mathbf{g} \times \mathbf{A}]\{\tilde{\mathbf{u}}^i\} \tag{20}$$

In a sine-dwell GVT, the modal mass and damping ratio are calculated from complex power curves determined over a small frequency range centered on the modal frequency. The complex power, in turn, is determined from the excitation force and the acceleration of the structure at the excitation point. In a phase separation test the modal parameters are calculated from the transfer function of excitation force to acceleration at the excitation point. If the impedance head or accelerometer measuring the acceleration at the excitation point was allowed to rotate with the structure, the measured acceleration would be affected by gravity as indicated by Eq. (16). At low frequencies the measured acceleration, and consequently the modal parameters, would be significantly affected. It is therefore important to prevent the impedance head or the accelerometer measuring the response at the excitation point from rotating when extracting low frequency modes. One possibility is to mount the impedance head on the exciter armature rather than on the structure.

From Eq. (20) it can be seen that the magnitude of the gravity correction is proportional to the inverse of the square of the modal frequency. The question arises as to what should be regarded as low frequency. As a general guideline, the modal frequency should be compared to the frequency of a pendulum with a length equal to a characteristic length of the test piece. At that frequency, the apparent modal displacement due to gravity would be of the same order of magnitude as the actual displacement.

2.3 Approximate Method to Determine Quadratic Mode Shape Components. The method for directly measuring quadratic mode shape components is only applicable to sine-dwell testing and requires sensors that measure down to zero frequency; in addition to signal processing which is not implemented in typical GVT systems. The finite element-based methods of Segalman et al. [4,5] and Van Zyl and Mathews [6] are only applicable if a validated finite element model of the structure is available. An approximate method for estimating the quadratic mode shape components from the linear components was therefore developed. This method also makes use of the node coordinate and connectivity data that is customarily generated for a GVT and, commensurate with the gravity correction procedure, also requires that each node and all its neighbors may not be collinear.

The linearized representation of the displacement of a structural element that experiences rotation implies an extension of the element that is proportional to the square of the angle of rotation. The finite element-based method of Van Zyl and Mathews [6] specifies that the elastic potential energy associated with this extension is minimized by the addition of the quadratic mode shape component, consistent with the restraints of the model. In the present method we treat the connections used for visualizing the mode shapes as if they were inextensible structural elements. The method specifies that the extension of each connection, due to its rotation in each mode shape, is canceled by the addition of the quadratic mode shape component.

The inextensibility conditions are generally not sufficient to obtain a unique solution for the quadratic mode shape component. They are supplemented by introducing a nonphysical rotational stiffness at each attachment of a connection to a node. Since the set of equations is solved in a least-squares sense, the rotational

stiffness conditions take the form of equations specifying that the rotation of each connection connected to a node is equal to the rotation of the node itself. These equations must be given an appropriate weighting in order to resolve conflicting inextensibility and rotational stiffness conditions realistically.

Over-restraining of a structure may also give rise to conflicting inextensibility conditions. In the absence of any physical stiffness information, conflicting inextensibility conditions cannot be resolved in a consistent manner. Therefore, the method is strictly only applicable to cantilevered structures.

The quadratic displacements at each node are determined from a set of linear equations. The set of equations are constructed and solved as follows:

(1) *For each connection, the quadratic mode shape component must cancel the extension due to the rotation of the connection.*
The rotation of the connection is determined from

$$\mathbf{r} = \underline{\ell} \times \left(\mathbf{u}_2^i - \mathbf{u}_1^i\right) \Big/ |\underline{\ell}|^2 \tag{21}$$

Where the subscripts 1 and 2 refer to the nodes at either end of the connection and $\underline{\ell}$ is the vector from the first end point to the second end point. The quadratic extension of the connection in mode i is given by

$$e = \frac{1}{2}|\mathbf{r}|^2 |\underline{\ell}| \tag{22}$$

The equation for the connection requires that this extension of the connection must be cancelled by the quadratic mode shape component:

$$\underline{\ell} \cdot \left(\mathbf{g}_2^{ii} - \mathbf{g}_1^{ii}\right) \Big/ |\underline{\ell}| = -e \tag{23}$$

(2) *At each node, the rotation of each connection in the quadratic mode shape component must be equal to the rotation of the node itself.*
The condition is applied in two orthogonal directions normal to the connection. The rotation of the node in the quadratic mode shape component is determined from the linear combination in Eq. (18) and the rotation of each connection is determined from

$$\mathbf{r} = \underline{\ell} \times \left(\mathbf{g}_2^{ii} - \mathbf{g}_1^{ii}\right) \Big/ |\underline{\ell}|^2 \tag{24}$$

(3) *The system of equations is solved in a least-squares sense.*
The system of equations is generally over-specified and some restraint conditions are also required for a solution. Individual degrees of freedom at selected nodes can be set equal to zero for this purpose.

If the coupled quadratic mode shape component corresponding to modes i and j is required, the individual quadratic components $\mathbf{g}^{ii}$ and $\mathbf{g}^{jj}$ are first determined as described above. An artificial linear mode shape is generated by summing the two linear mode shapes and the quadratic mode shape component $\tilde{\mathbf{g}}$ of this mode is determined by the same procedure. Expanding Eq. (4) of Dohrmann and Segalman [2] for two modes, and noting that $\mathbf{g}^{ij}$ and $\mathbf{g}^{ji}$ are identical, the quadratic component of the artificial mode is given by

$$\tilde{\mathbf{g}} = \mathbf{g}^{ii} + \mathbf{g}^{jj} + 2\mathbf{g}^{ij} \tag{25}$$

The coupled quadratic mode shape component $\mathbf{g}^{ij}$ can therefore be calculated from

$$\mathbf{g}^{ij} = \frac{1}{2}\left(\tilde{\mathbf{g}} - \mathbf{g}^{ii} - \mathbf{g}^{jj}\right) \tag{26}$$

3 Implementation

The method for measuring quadratic mode shape components was implemented using a data acquisition processor (DAP) board installed in a personal computer (PC) and the associated signal conditioning equipment. The layout of the GVT system is illustrated in Fig. 2.

The excitation system consists of a software signal generator running as a process on the DAP board, a custom analog bandpass filter for overdrive protection, an amplifier, and an electrodynamic exciter. An impedance head is used to measure the input force and driving point response for excitation control. Data acquisition is also performed by a process running on the DAP board. The Fourier coefficients for each channel are determined and these are passed to the main process running on the PC. The coefficients for each channel have a common but arbitrary phase reference. There will generally be sine as well as cosine terms in the Fourier series at this stage.

The main program applies the transfer function of each sensor to the Fourier coefficients to obtain responses in engineering units and then applies a phase reference based on the excitation force to all channels. The complex power method is used to determine the modal frequency and other modal parameters. The excitation frequency is then set to the modal frequency and the Fourier coefficients of each response channel, after applying the sensor transfer functions and phase reference, are recorded. There should be predominantly cosine terms in the Fourier series at this stage. Thereafter the excitation is stopped and rest readings are taken. The rest readings eliminate the need to know the zero-g offsets of the accelerometer outputs and the exact value of g. The linear and quadratic mode shape components are then calculated according to the equations derived above.

4 Application

The procedure for direct measurement of quadratic mode shape components was applied to the ground vibration testing of a T-tail flutter model. The experimental setup is shown in Fig. 3 and illustrates the customary practice of mounting the impedance head on the structure. The model is mounted on a circular base which can rotate around a vertical axis against a spring system. However, the base was restrained for the purpose of this test.

The method for estimating quadratic mode shape components from the linear components was applied to the first torsion mode of a rectangular plate. The linear mode shape component was calculated using FEA. This linear mode shape component was used as input to the method and the result compared to the quadratic mode shape component calculated using the FEA-based method of Van Zyl and Mathews [6].

The methods for correcting GVT results for the effect of gravity and for estimating the quadratic mode shape component from the linear component were applied to the ground vibration testing of a pendulum. The experimental setup is shown in Fig. 4 and illustrates the recommended practice of mounting the impedance head on the exciter armature for low frequency modal testing.

4.1 Direct Measurement of Quadratic Mode Shape Components. The model was instrumented with eight triaxial MEMS accelerometers, which measure down to zero frequency. Six were mounted on the horizontal stabilizer and two at midheight on the fin. The excitation force was applied at midheight of the fin, close to the trailing edge. Both the fin bending and torsion modes could be adequately excited from this position. The excitation force and acceleration at the driving point were measured using a piezoelectric impedance head. The fin bending frequency was 7.2 Hz and the fin torsion frequency was 15.1 Hz.

Because of the symmetry of the model, the path of any point on the stabilizer in the fin torsion mode should be a circular arc around a vertical axis through the center of the stabilizer. The experimentally determined paths of the measurement nodes in the

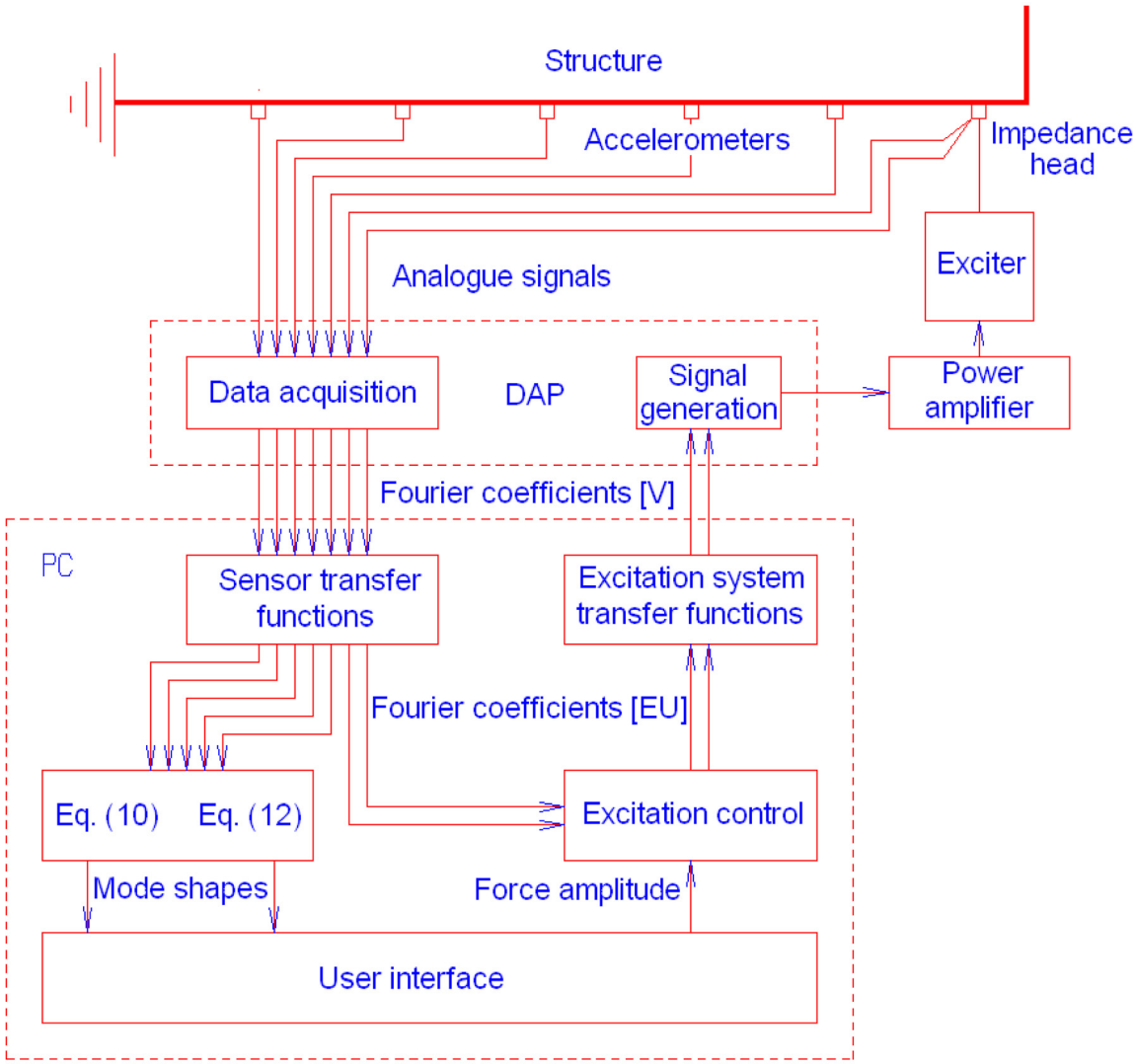

Fig. 2 Layout of the sine-dwell GVT system

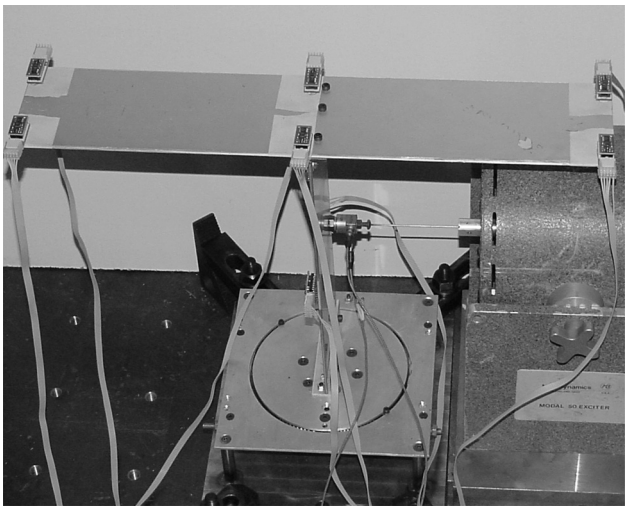

Fig. 3 Experimental setup for the T-tail GVT

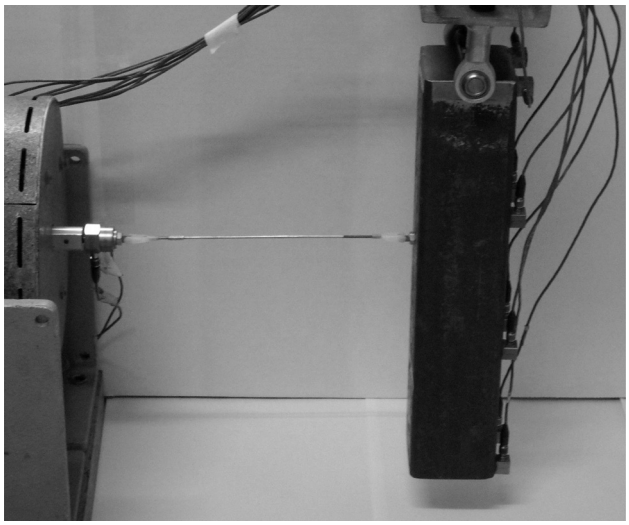

Fig. 4 Experimental setup for the pendulum GVT

fin torsion mode are compared to the exact circular arcs as well as the finite element-based method of Van Zyl and Mathews [6] in Fig. 5. The displacements are scaled up by a factor of 27 relative to the amplitude at which the mode shape was measured. The correlation between the circular arcs and both parabolic approximations is good.

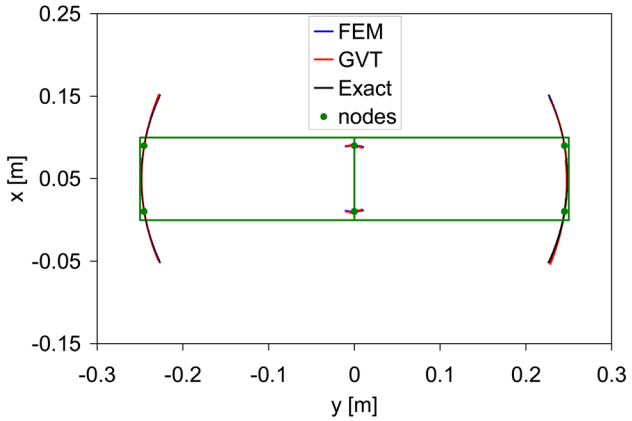

Fig. 5 T-tail flutter model fin torsion mode, top view

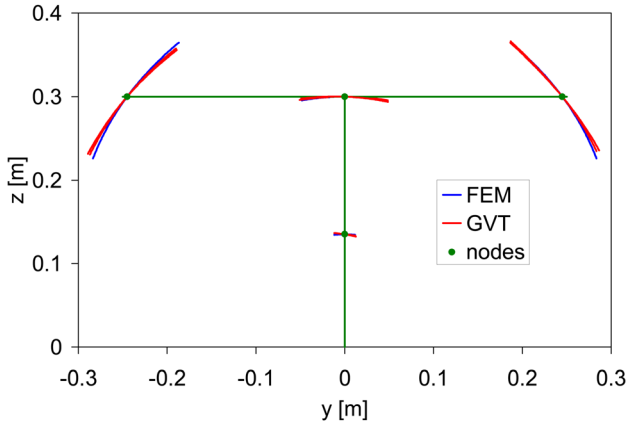

Fig. 6 T-tail flutter model fin bending mode, rear view

The experimentally determined paths of the measurement nodes in the fin bending mode are compared to the FE-based method of Van Zyl and Mathews [6] in Fig. 6. There is no simple exact path as for the torsion mode. The displacements are scaled up by a factor of 14 relative to the amplitude at which the mode shape was measured. The correlation between the two parabolic approximations is reasonable.

4.2 Estimation of the Quadratic Mode Shape Component of a Rectangular Plate in Torsion. The procedure for estimating the quadratic mode shape component from the linear component, and the effect of the weighting of the nonphysical rotational stiffness conditions, is illustrated for a rectangular plate in torsion. The plate has an aspect ratio of 2 and is clamped along one short edge. The reference solution was calculated using the FEA method of Van Zyl and Mathews [6]. Figure 7 can be interpreted as the view normal to the plate vibrating in its first torsion mode at an amplitude of approximately 45 deg twist at the free end.

The solution with equal weighting implies that the same weight was attached to unit strain (change in length equal to the length of the connection) and 1 rad rotation of a connection relative to the node rotation. In the "low weight" solution the weighting of the rotation was reduced by a factor of 10. Torsion of a plate involves significant in-plane shear deformation, a fact which can be appreciated by twisting a sheet of paper. In this example, the equal weighting of the extension and rotation conditions limits the calculated shear deformation to less than the shear deformation that occurs in reality. In the low weight solution the shear deformation is still being limited by the rotation condition, simulating the shear stiffness of the plate. Reducing the weighting further results in greater calculated shear deformation than occurs in reality. When

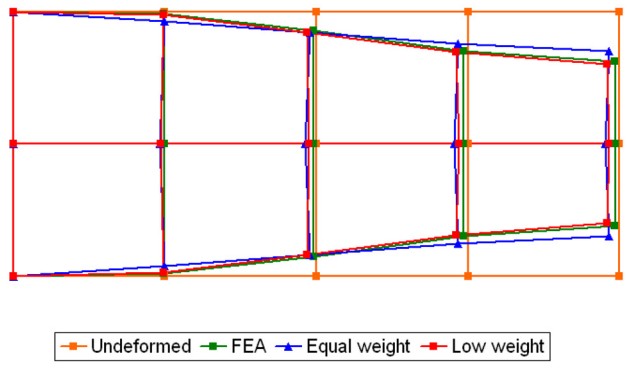

Fig. 7 Quadratic mode shape component of the first torsion mode of a rectangular plate

the procedure is applied to planar structures, e.g., aircraft wings or empennages, the weighting of the rotation condition has to be adjusted to obtain realistic results for torsion modes. In the case of bending modes of planar structures, the rotation condition has no effect on the solution because there is no in-plane shear deformation.

4.3 Gravity Correction and Estimation of Quadratic Mode Shape Component. The fundamental mode of a pendulum was measured in a sine-dwell ground vibration test using a piezoelectric impedance head and single-axis piezoelectric accelerometers, which do not measure down to zero frequency. The pendulum consisted of a steel bar of 300 mm in length with a slightly rounded ($r \approx 5$ mm), 60 mm by 60 mm cross section. The excitation position was 0.125 m below the rotation axis, which coincided with the top of the steel bar. Local gravitational acceleration was 9.78 m/s^2. The theoretical frequency was 1.107 Hz and the theoretical mass moment of inertia about the rotation axis was 0.254 kg m^2. The measured frequency and moment of inertia were 1.115 Hz and 0.228 kg m^2, respectively. The theoretical apparent rotation axis was 0.202 m below the actual rotation axis.

The pendulum was instrumented with two rows of four accelerometers each along its length. The measured displacements were first corrected for gravity according to Eq. (20) after which the quadratic mode shape component was added according to the method described in Sec. 2.3. The measured and corrected

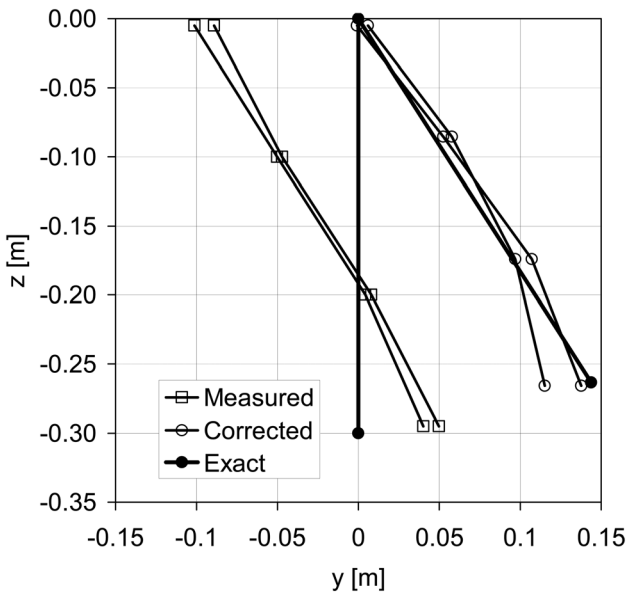

Fig. 8 Measured and corrected mode shapes of the pendulum

displacements are shown in Fig. 8 for an amplitude of 0.5 rad. The corrected rotation point is reasonably accurate, within the uncertainty of the original measurement. It is apparent that the measurement errors are amplified by the gravity correction, however, the overall error in the mode shape is significantly reduced.

5 Conclusion

It seems feasible to measure quadratic mode shape components using a sine-dwell GVT system provided that the steady component of the acceleration is measured and the signal processing algorithm is expanded to calculate the mean value and the second harmonic of acceleration.

It should be noted that harmonics in the accelerometer outputs can be caused by structural nonlinearities as well as the curved trajectory of the accelerometer. The method described here should therefore be applied with discretion. On the other hand, higher harmonics in accelerometer outputs should not always be ascribed to structural nonlinearities.

The approximate method for calculating the quadratic mode shape component from the linear component was demonstrated for a rectangular plate in torsion. The method is strictly only applicable to cantilevered structures.

The method of correcting low frequency GVT results for the effect of gravity (i.e., the effect on the measurement) was illustrated for a pendulum and is applicable to any structure provided that the layout of the accelerometers allows for the determination of the rotation of each node.

A FORTRAN code implementing the methods for estimating quadratic mode shape components from the linear components and for gravity correction is available from the authors.

References

[1] Segalman, D. J., and Dohrmann, C. R., 1990, "Dynamics of Rotating Flexible Structures by a Method of Quadratic Modes," Technical Report No. SAND-90-2737, Sandia National Laboratories, Albuquerque, NM.

[2] Dohrmann, C. R., and Segalman, D. J., 1996, "Use of Quadratic Components for Buckling Calculations," Technical Report No. SAND-96-2367C, Sandia National Laboratories, Albuquerque, NM.

[3] Van Zyl, L. H., and Mathews, E. H., 2011, "Aeroelastic Analysis of T-tails Using an Enhanced Doublet Lattice Method," J. Aircraft, **48**(3), pp. 823–831.

[4] Segalman, D. J., and Dohrmann, C. R., 1996, "A Method for Calculating the Dynamics of Rotating Flexible Structures, Part 1: Derivation," ASME J. Vib. Acoust., **118**, pp. 313–317.

[5] Segalman, D. J., Dohrmann, C. R., and Slavin, A. M., 1996, "A Method for Calculating the Dynamics of Rotating Flexible Structures, Part 2: Example Calculations," ASME J. Vib. Acoust., **118**, pp. 318–322.

[6] Van Zyl, L. H., and Mathews, E. H., 2012, "Quadratic Mode Shape Components From Linear Finite Element Analysis," ASME J. Vib. Acoust., **134**(1), pp. 014501.

[7] Lacarbonara, W., Rega, G., and Nayfeh, A. H., 2003, "Resonant Non-linear Modes. Part I: Analytical Treatment for Structural One-Dimensional Systems," Int. J. Non-Linear Mech., **38**, pp. 851–872.

[8] Lacarbonara, W., and Rega, G., 2003, "Resonant Non-linear Modes. Part II: Activation/Orthogonality Conditions for Shallow Structural Systems," Int. J. Non-Linear Mech., **38**, pp. 873–887.